Elliptic and Hyperbolic Dielectric Lens Antennas in mm-Waves

Petr PIKSA, Stanislav ZVANOVEC , Petr CERNY

Dept. of Electromagnetic Field, Czech Technical University in Prague, Technicka 2, 166 27 Prague, Czech Republic

piksap@fel.cvut.cz, xzvanove@fel.cvut.cz, xcernyp1@fel.cvut.cz

Abstract. *Dielectric lenses can substantially improve antenna parameters, especially the planarity of radiated waves and the antenna gain. The paper deals with their application in millimeter-wave band. The main goal concerns the introduction of characteristics and differences between the most commonly used types of dielectric lens antennas, i.e. elliptic and hyperbolic. Their particular features as well as behavior of radiating systems incorporating the lenses are investigated. Specific features of these lenses are discussed for both, near-field and far-field based on simulation and measurement results.*

Keywords

Dielectric lens antennas, elliptic, hyperbolic, millimeter wave antennas, millimeter wave measurements.

1. Introduction

Dielectric lenses transform an electromagnetic wave radiated by an antenna into a plane wave or they focus a radiated beam into narrow space similarly to the Gaussian beam propagation approach used in optics. Contrary to the optical region, where analytical approaches are based on the ray optics, in quasi optical and microwave region, the radiated beam tends to diverge faster as the distance grows. Therefore proposed optical geometric lenses should be analyzed in both near-field (where the deviation of beam can be clearly distinguished from the transformation of waveforms) and far-field (where the diffraction, reflections and other negative influences can be observed).

Some preliminary results of electromagnetic simulations dealing with dielectric lenses were involved as indirect results in authors' publications [1] and [2]. Contrary to them, this paper summarizes the authors' experience acquired through the research accomplished within the Centre of Basic Research - Centre for Quasi-Optical Systems and Terahertz Spectroscopy – KVASTES, where the research was carried out in order to incorporate the lenses into the Fabry-Perot resonator (used in the microwave spectroscopy). Several types of dielectric lenses were analyzed in the project in order to attain a proper irradiation of the coupling foil placed inside the resonator [3], and also to reach the required distribution of the transmitted waveform [4].

This paper is structured as follows: the introduction of the most frequently employed types of dielectric lenses (namely elliptic and hyperbolic) is followed by investigation and analysis of their specific features in near-field as well as far-field that are based on simulation and measurement results.

2. Overview of Dielectric Lens Antennas

As mentioned above, dielectric lenses transform spherical waves into planar waveforms. In addition, they increase the antenna aperture and, accordingly, the antenna gain. Both analyzed types of lenses - elliptic and hyperbolic - proved to have specific advantages and drawbacks that are going to be detailed in the following text. Other lens types were not taken into consideration (for more information see e.g. [5] or [6], [7]).

Given its low loss in millimeter wave band, the simulated and realized lenses were made of teflon (PTFE Polytetrafluoroethylene). The measured material parameters are listed bellow: permittivity $\varepsilon_r = 2.024$ and loss factor $\mathrm{tg}\,\delta = 0.0074$ at the frequency of 40 GHz and permittivity $\varepsilon_r = 2.044$ and loss factor $\mathrm{tg}\,\delta = 0.0041$ at the frequency of 90 GHz.

2.1 Elliptic Lens

Geometry of an elliptic lens can be described by two curves. The inner (irradiated) shape of the lens is spherical. It is described by the radius ρ_1, while the outer shape is elliptic and can be described in polar coordinates as [8]

$$\rho_2(\psi) = \frac{(n-1)\,f}{n-\cos\psi} \tag{1}$$

where n represents the refractive index of dielectric material ($\varepsilon_r = n^2$) and f stands for the focal distance of the

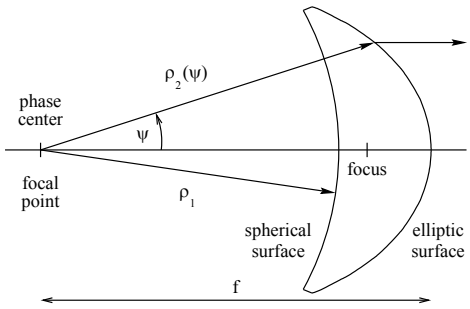

Fig. 1. Geometry of the elliptic lens.

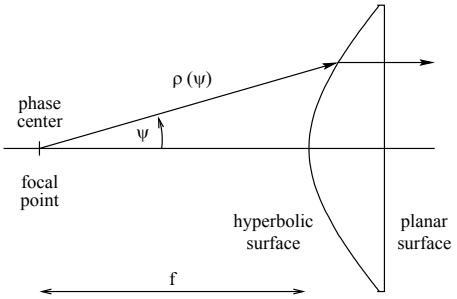

Fig. 3. Geometry of the hyperbolic lens.

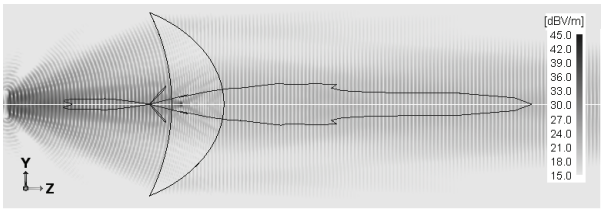

Fig. 2. Modeled distribution of waveforms and far-field radiation pattern in case of the elliptic lens at 90 GHz.

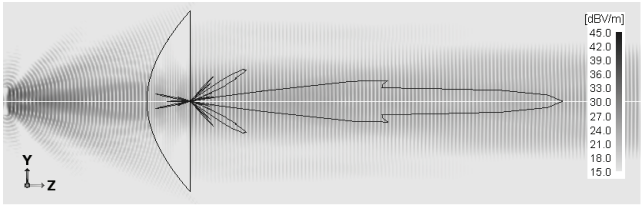

Fig. 4. Modeled distribution of waveforms and far-field radiation pattern in case of the hyperbolic lens at 90 GHz.

lens. The particular parameters and shapes of the lens are illustrated in Fig. 1. The phase center of the irradiating antenna has to be placed in the focal point of the lens so that the spherical electromagnetic wave incides on the inner surface of the lens.

The inner surface of the elliptic lens represents an ideal case for proper irradiation by a source antenna and therefore the lens is able to create more homogenous wave than the hyperbolic one, whose more distant parts of the inner surface can be less irradiated [8]. Since the elliptic lens can be irradiated more effectively, a higher antenna gain can be reached.

In order to validate and test their features, several dielectric lenses have been developed. The following text comprises the example that is based on the designed elliptic lens having the diameter of 80 mm and focal distance of 110 mm.

The modeled distribution of electric field (E-plane) around the elliptic lens is depicted in Fig. 2. The modeling was performed using the commercial software FEKO. As it is apparent from the waveforms, the near-field behind the lens is homogenous and the emitted wave is exceptionally planar. The far-field, represented by the radiation pattern given in Fig. 2, explicitly determines directions, in which the undesirable reflections and diffractions arise.

The main disadvantage of the elliptic lens - backward radiation - can be distinguished from the far-field characteristic. It originates from the perpendicular reflection of electromagnetic wave from the inner surface of a dielectric lens (i.e. the boundary between the air and dielectric material) towards the source.

2.2 Hyperbolic Lens

The virtue for the utilization of a hyperbolic lens consists mainly in its simple shape and therefore easier development. Its inner shape can be expressed in polar coordinates (see [8]) as:

$$\rho(\psi) = \frac{(n-1)\,f}{n\,\cos\psi - 1}. \tag{2}$$

The particular parameters of the lens are demonstrated in Fig. 3. For the subsequent study the designed lens with the diameter of 80 mm and the focal distance equaling 75 mm was selected.

Fig. 4 illustrates the modeled electric field distribution (E-plane) as transformed by this lens. As far as the crucial weaknesses of hyperbolic lenses are concerned, it is necessary to highlight worse irradiation of the most distant parts of surface (taken from the axis of propagation) and also diffraction over the lens edges. The latter gives rise to the undesirable side-lobes around 30 degrees off axis (see the far-field radiation pattern in Fig. 4).

When it is compared with the simulation results a better planarity of the waveforms behind the lens can be noticed in case of the elliptic lens, where the total phase error of electric field distribution in the perpendicular cut taken at the distance of 0.2 m reaches $\pi/18$ in the radius of 25 mm off axis. This corresponds to the plane wave distortion of $\lambda/36$. Contrary to that, the total phase error of $\pi/6$ (the plane wave distortion being equal to $\lambda/12$) was observed behind the hyperbolic lens.

3. Positioning of Antenna

In order to match the appropriate position of the antenna phase center with the focal point of the particular lens, a study of the frequency dependence of antenna gain on the placement of antenna in front of the lens was accomplished. The results for the elliptic lens as well as for the hyperbolic lens are depicted in Fig. 5 and Fig. 6, respectively. The offset (i.e. the parameter indicated on the x-axis) represents a shift between the phase center and the intersection of the horn antenna (it means an imaginary apex of the horn on the axis of propagation). It is vital to take into account a slight frequency shift of the gain maximum dependency on the position of the antenna in front of the lens.

It is necessary to emphasize the assumption that the plane wave created behind the lens can be exactly fulfilled only in the maximum gain. For measurements discussed in following sections, the positions corresponding to the maximum of gain at 90 GHz were chosen. These can be expressed by the offset equal to 8.6 mm in case of the elliptic lens and 9.2 mm in case of the hyperbolic lens.

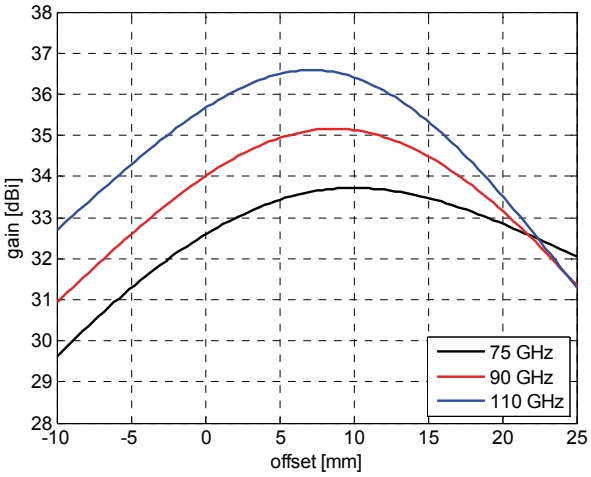

Fig. 5. Positioning of the horn antenna in front of the elliptic lens.

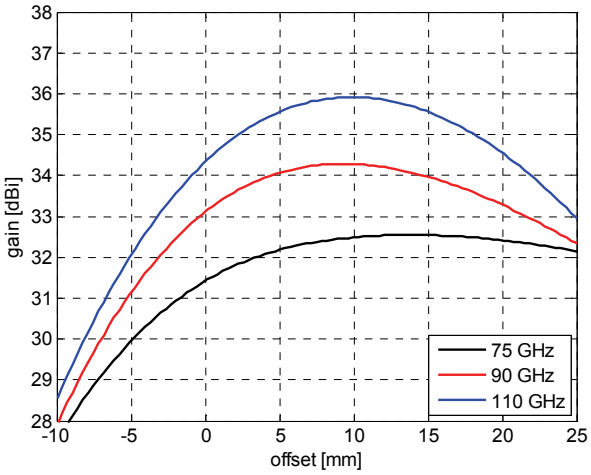

Fig. 6. Positioning of the horn antenna in front of the hyperbolic lens.

The asymmetric performance of the achieved gain in dependence on the position of the antenna can be explained by a different irradiation of the inner shapes of both lenses. In case of the hyperbolic lens, over-radiation is more evident since distant parts (off axis) of the inner surface are farther from the focal point than in case of the elliptic lens.

Unlike the latter case, from the point of view of the theory of Gaussian beam coupling to radiating system [9], the mentioned phase center offset of the rectangular horn antenna (15.4 x 11.2 x 19 - width x height x depth, all in mm) is equal to 6.2 mm.

4. Near-field Measurement

Real non-homogeneities behind the lenses can be classified and verified only in case they are based on near-field measurements.

The following instruments were employed in the measurement: Agilent 8257D microwave synthesizer, whose frequency was tripled using the Wisewave FMP-KF310-01 tripler and transmitted by the waveguide (PWS-1004-01) fed horn antenna (for dimensions see Section 3). In addition, the radiation was detected by the probe (truncated waveguide WR-10) and analyzed by the Agilent Spectral Analyzer E4440A, whose frequency range was extended up to the 75–110 GHz range using the external Agilent 11970W harmonic mixer. Our department is not equipped with a vector network analyzer capable of measuring in the frequency bands exceeding 50 GHz. Hence the planarity (phase value) could not be verified via measurement and merely a scalar measurement was performed in order to get information about the homogeneity of the radiated beam.

The 2D scanning system (see Fig. 7), with the step of 1 mm in y-axis and step of either 30 mm (for z = 0 to 300 mm) or 50 mm (for z = 300 to 500 mm) was employed in z-axis. Fig. 8 and Fig. 9 indicate results of the measured power distribution (E-plane) behind the dielectric lenses. To reach these distributions, 16 measuring scans had to be performed. The near-field area in our measurements was considered to be extended up to 500 mm, which corresponds to 150 wavelengths at the frequency of 90 GHz.

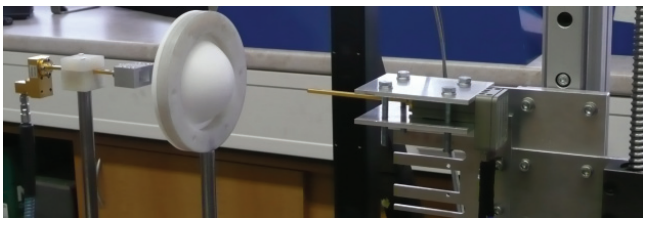

Fig. 7. Arrangement of the 2D scanning system; harmonic mixer with waveguide probe, elliptic lens, horn antenna, waveguide and tripler in near-field measurement.

There are obvious drops in power distribution behind the lenses, resulting from the diffraction of the incident wave at the edge of the lens. Contrary to the optics, lenses

have dimensions not over-sizing hundreds of wavelengths in millimeter waves. Consequently, a purely geometrical optic approach is inaccurate and a higher deformation of the field behind the lenses can be noticed. Owing to the agreement with the Gaussian beam, a degree of beam deformation behind the lenses can be interpreted.

The electric field distribution of the Gaussian beam is determined as stated in [10]

$$E(r,z) = E_0 \frac{w_0}{w(z)} e^{-j[kz-\psi(z)]} e^{-j\frac{k\,r^2}{2\,R(z)}} e^{-\frac{r^2}{w^2(z)}} \quad (3)$$

where

$$w^2(z) = w_0^2 \left[1 + \left(\frac{\lambda\, z}{\pi\, w_0^2}\right)^2\right], \quad (4)$$

$$R(z) = z \left[1 + \left(\frac{\pi\, w_0^2}{\lambda\, z}\right)^2\right], \quad (5)$$

$$\psi(z) = \tan^{-1} \frac{\lambda\, z}{\pi\, w_0^2}, \quad (6)$$

$w(z)$ is the beam radius, w_0 represents the beam waist, $\psi(z)$ stands for the phase variation and $R(z)$ embodies the radius of curvature.

The agreement with the Gaussian beam can then be enumerated by a normalized cross-correlation function as a factor reaching values from 0 to 1. The latter is attained in case of the total agreement. Tab. 1 summarizes the resulting comparisons for hyperbolic and elliptic lenses in cases where the maxima for distributions at 0.15 m, 0.3 m and 0.5 m behind lenses were averaged. The measurement revealed a higher beam deformation especially behind the elliptic lens.

	Hyperbolic lens		Elliptic lens	
	Modeling	Measurement	Modeling	Measurement
Agreement factor	0.9955	0.9844	0.9951	0.9676
Optimized w_0 [mm]	25	24	25	30

Tab. 1. Maximum of agreement between measured and Gaussian beam distribution with optimized beam waist w_0.

5. Far-field Measurement

All the designed antennas were also validated by far-field measurements in the anechoic chamber in the distance of 3.8 m at 90 GHz according to the criteria for the far-field region [8].

As it is clear from Fig. 10, the antenna with the elliptic lens attains higher level of gain especially in the lower measured frequency band (i.e. 50 - 75 GHz). There

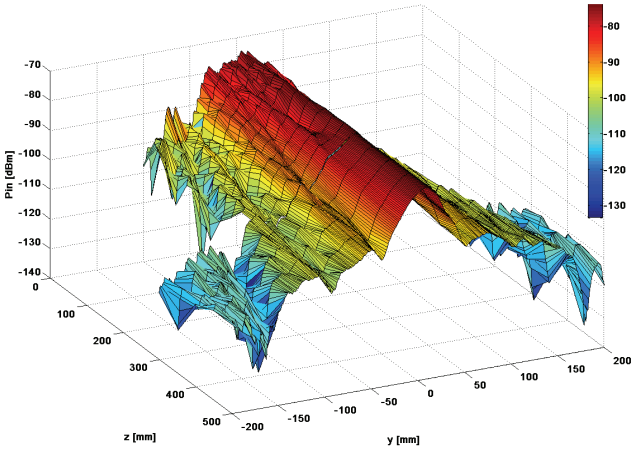

Fig. 8. Measured near-field (E-plane) behind the elliptic lens at 90 GHz.

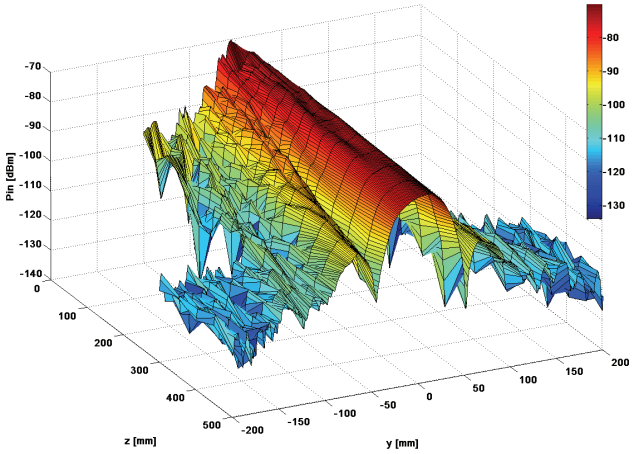

Fig. 9. Measured near-field (E-plane) behind the hyperbolic lens at 90 GHz.

is obviously only a slight difference in gains within the higher frequency band. This can be attributable to losses of transmitted electromagnetic wave in dielectric material of the elliptic lens. This phenomenon gives proof of a higher depth in the axis of propagation. Alternatively, it can result from manufacturing inaccuracy, incurred during the turning operation on a lathe, when the soft dielectric material might have clamped. Two reference horn antennas, designed for the ranges from 50 to 75 GHz and 75 to 110 GHz, were utilized in accordance with the standardized waveguide dimensions.

Fig. 11 depicts radiation patterns of the radiating system consisting of an antenna and a particular lens, measured by the reference horn antenna. As for these characteristics, it is possible to point out the emergence of side lobes. Please note that the difference between side lobes of the horn antenna and the antenna with particular lens caused by reflections from the lens reaches up to 10 dB. Indeed, in real situation, more side lobes can be distinguished in comparison with simulations mentioned in Section 2.1 (see Fig. 2 and Fig. 4) where E-plane was depicted because, in principle, the rectangular horn antenna has side lobes only in the E-plane. In the far field, H-plane

was measured in order to avoid the influence of side lobes of the horn antenna on resulting measurement of reflections and diffractions from the lenses.

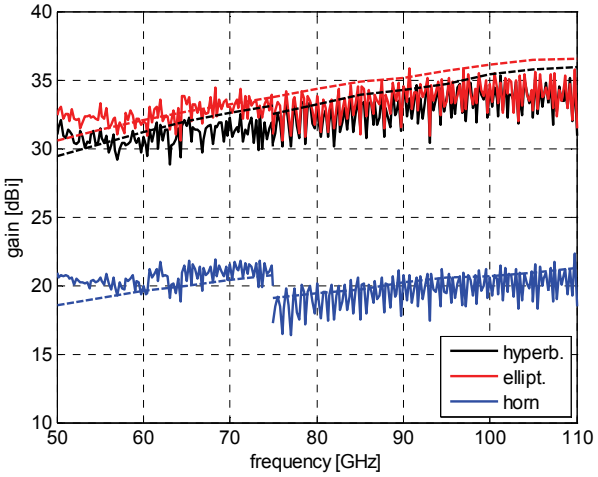

Fig. 10. Measured (solid line) and modeled (dashed line) gain of horn antennas and horn antennas with either elliptic or hyperbolic lens.

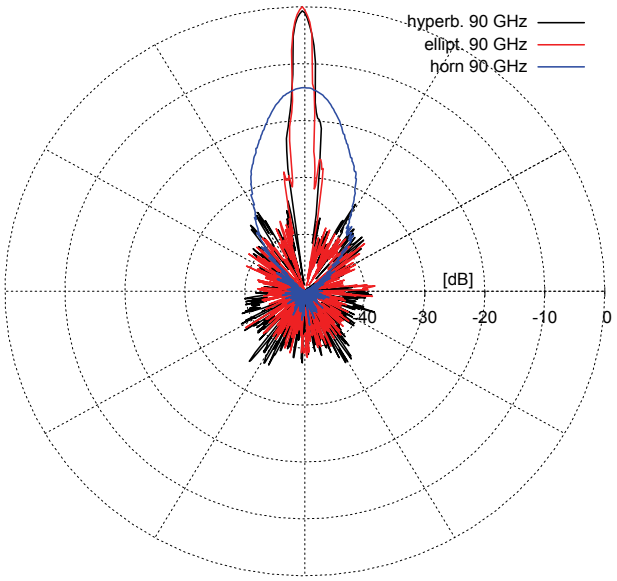

Fig. 11. Measured radiation pattern (H-plane) of horn antenna and horn antenna with elliptic or hyperbolic lens at 90 GHz, normalized to maximum gain of elliptic lens.

6. Conclusions

By means of simulations and measurements, several specifics of dielectric lens utilization were discussed. The assumptions related to the elliptic and hyperbolic lenses were partially proved. According to the tests, the elliptic lens provides a better planarity of the transformed wave in the model. Nonetheless, it was found out that in the higher frequency band (where the beam was non-deformed and antenna gain reached up to 36.5 dBi at the frequency of 110 GHz), the features of the elliptic lens did not entirely correspond to the assumptions taken from the model. These inaccuracies arose from manufacturing misalignments, for the chosen dielectric material proved to have almost frequency-independent electrical parameters.

Acknowledgements

The research was financed by the Ministry of Education, Youth and Sports of the Czech Republic within the Research Program LC06071. For the experimental activities, the support from the Czech Science Foundation (GACR 102/08/P346) was gained, while the measurements were financed though the project “Research in the Area of the Prospective Information and Navigation Technologies” (MSM 6840770014).

References

[1] ZVANOVEC, S., PIKSA, P., CERNY, P., MAZANEK, M., PECHAC, P. Gas attenuation measurement by utilization of Fabry-Perot resonator. In *Proceedings of the 2nd European Conference on Antennas and Propagation*. Edinburgh (UK), 2007.

[2] PIKSA, P., CERNY, P., ZVANOVEC, S., MAZANEK, M., URBAN, S. Dielectric lens utilization for Fabry-Perot resonator optimal coupling. In *Proceedings of the European Microwave Week 2008 "Bridging Gaps" Conference*. Amsterdam (Netherlands), 2008, p. 955 - 958.

[3] ZVANOVEC, S., CERNY, P., PIKSA, P., KORINEK, T., PECHAC, P., MAZANEK, M., VARGA, J., KOUBEK, J., URBAN, S. The use of the Fabry-Perot interferometer for high resolution microwave spectroscopy. *Journal of Molecular Spectroscopy*, 2009, vol. 256, no. 1, p. 141 - 145.

[4] PIKSA, P., CERNY, P., ZVANOVEC, S., MAZANEK, M. Optimization of beam focusing into the Stark´s cell for mm-wave spectroscopy. In *Proceedings of the 2nd European Conference on Antennas and Propagation*. Edinburgh (UK), 2007.

[5] JOHNSON, R. C. *Antenna Engineering Handbook*, 3rd ed. New York: McGraw-Hill, 1993, Ch.16.

[6] WESTCOTT, B. S., BRICKELL, F. General dielectric-lens shaping using complex co-ordinates. *IEE Proceedings on Microwaves, Antennas and Propagation*, 1986, vol. 133, p. 122 - 126.

[7] LEE, J. Dielectric lens shaping and coma-correction zoning, part I: analysis. *IEEE Transactions on Antennas and Propagation*, 1983, vol. 31, p. 211 - 216.

[8] MILLIGAN, T. A. *Modern Antenna Design*, 2nd ed. New York: Wiley, 2005, p. 56, 448 and 451.

[9] GOLDSMITH, P. *Quasioptical Systems*. IEEE Press, 1998, p. 179.

[10] CHEN, C. L. *Elements of Optoelectronics & fiber optics*. Irwin, 1995, p. 51.

About authors...

Petr PIKSA was born in 1977. He received his M.Sc. degree in 2002 and Ph.D. degree in 2007 at the Czech Technical University in Prague. His interests are in the

field of planar antennas, modeling of electromagnetic field, quasi-optics, millimeter wave measurements and microwave spectroscopy measurements. He is a member of Radioengineering Society.

Stanislav ZVANOVEC was born in 1977. He received the M.Sc. degree in 2002, Ph.D. degree in 2006 and defended the habilitation thesis in 2010 at the Czech Technical University in Prague. To date, he is an associate professor at the Department of Electromagnetic Field at the CTU in Prague. His current research interests include electromagnetic wave propagation issues for millimeter wave band as well as quasioptical and free space optical systems. He is a member of IEEE, Radioengineering Society and head of the Commission F of the Czech National URSI Committee.

Petr CERNY was born in 1976. Czech Technical University in Prague awarded him M.Sc. and Ph.D. degrees in 2001 and 2008, respectively. His contemporary research activities are focused on the microwave spectroscopy, microwave circuits and antennas, ultra wideband devices and die bonding. He is a member of IEEE and Radioengineering Society.